AIAA JOURNAL
Vol. 32, No. 10, October 1994

# Technical Notes

*TECHNICAL NOTES are short manuscripts describing new developments or important results of a preliminary nature. These Notes cannot exceed 6 manuscript pages and 3 figures; a page of text may be substituted for a figure and vice versa. After informal review by the editors, they may be published within a few months of the date of receipt. Style requirements are the same as for regular contributions (see inside back cover).*

## Entrainment and Acoustic Variations in a Round Jet from Introduced Streamwise Vorticity

P. Surks* and C. B. Rogers†
*Tufts University, Medford, Massachusetts 02155*
and
D. E. Parekh‡
*McDonnell Douglas Research Laboratories, Saint Louis, Missouri 63166*

### I. Introduction

PREVIOUS research of the authors[1] examined changes in the acoustic and mass entrainment characteristics of a rectangular jet due to half-delta wing vortex generators. Unlike the tabs (e.g., Refs. 2–4), the half-delta wing vortex generators allow both co- and counter-rotating vortex pairs. This and previous work showed that counter-rotating pairs tend to produce more high-frequency noise and entrain less ambient fluid than their corotating counterparts. Further, the placement, sign, and strength of these streamwise vortices are critical in the overall mixing performance and noise control of the jet. In the rectangular nozzle, mixing increased by more than 35% and far-field jet noise reduced locally by as much as 3 dB. To examine the effect these generators have on the symmetry of a jet, the authors examined an axisymmetric jet cross section. The symmetry of the nozzle eliminated the effect of the corners and side walls of the rectangular nozzle, thus isolating the asymmetry induced by asymmetrical streamwise vorticity.

### II. Experimental Design and Methods

The experimental setup is identical to the one previously described in Rogers and Parekh.[1] The jet is a continuous, high-speed air jet with the nozzle pressure ratio actively controlled through a set of computer-actuated valves, to within ± 0.5%. After a 32:1 area ratio contraction, the air exits through a 6.35-cm-diam nozzle containing the half-delta wing generators (see Fig. 1). Holes were drilled every 45 deg around the circumference of the nozzle, 6.9 cm from the nozzle exit, for placement of the vortex generators. Two different generator shapes were examined: a 60- and a 70-deg internal angle half-delta wing. Both generator configurations had a nondimensional length of 0.4 diameters and are 0.16 mm thick.

Figure 2 shows schematically the various vortex configurations tested. These cases will be referred to by the direction of the common flow (flow between vortices, abbreviated CF) for the vortex pair cases and by the symmetry angle for the nonpair cases, for the remainder of the paper. The first two configurations were used to test the symmetry of the setup, since CF in/in is identical to CF out/out rotated 90 deg. The CF out/in case was chosen to examine an asymmetrical induced vortical flow, and the two symmetry cases show the effect of all generators with the same sign.

#### Mixing Measurements

We used the mixing effectiveness outlined in Rogers and Parekh[1] as a semiquantitative mixing measurement. Mixing effectiveness measurements were made by effectively measuring the concentration of smoke particles with a video camera and a light sheet; thus, this method is unable to distinguish between entrained and mixed flow but nonetheless allows a semiquantitative comparison. This mixing effectiveness is defined as

$$\eta = \frac{\text{average}\langle \text{pixel values within } \mathcal{R} \rangle}{\text{average}\langle \text{pixel values outside } \mathcal{R} \text{ but in the sheet} \rangle} \quad (1)$$

where $\mathcal{R}$ is the area of the picture under examination. Thus, a fully mixed jet is uniformly white and, therefore, the effectiveness is 1. Surks et al.[5] showed about an overall 10% uncertainty in the mixing effectiveness.

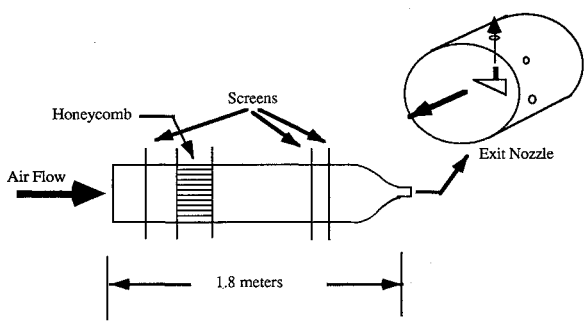


**Fig. 1 Jet schematic.**

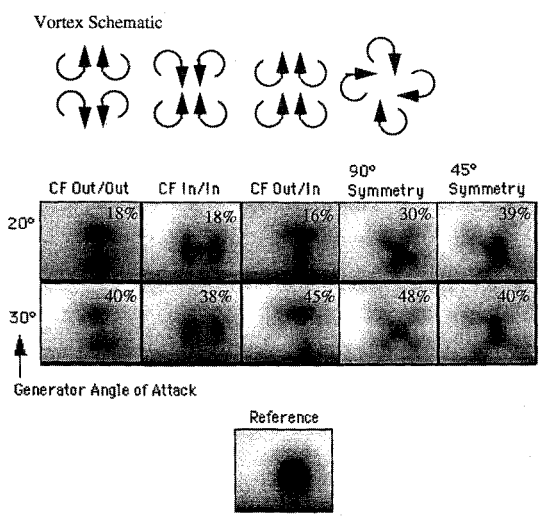


**Fig. 2 Flow visualization at $x/d = 6.68$.**

Received March 3, 1993; revision received Jan. 14, 1994; accepted for publication May 6, 1994. 

*Student, Department of Mechanical Engineering. Member AIAA.
†Assistant Professor, Department of Mechanical Engineering. Member AIAA.
‡Scientist, McDonnell Douglas Aerospace. Member AIAA.

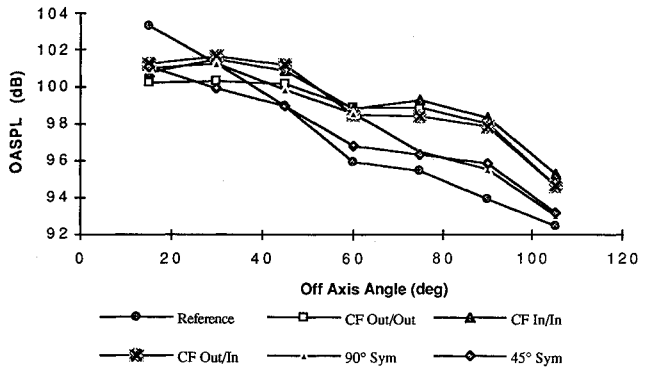


**Fig. 3 Increase in decibels over the reference case.**

### Acoustic Measurements

All acoustic measurements were taken with seven Brüel and Kjaer Model 4135 condenser microphones placed in the far field of the jet. The microphones were arranged in a single azimuthal plane radially around the jet from 15 to 105 deg, 26 jet diameters away from the nozzle exit. Azimuthal measurements were made by rotating the jet plenum and exit rather than the microphones. The walls of the test cell are covered πwith 10-cm-thick Sonex foam, and the microphones are flat to ± 0.5 dB in the frequencies of interest. Further, all microphones were calibrated daily with a Brüel and Kjaer pistonphone. The microphone voltage signals were conditioned with a brickwall, low-pass filter at 23 kHz, and sampled at 51.2 kHz. All acoustic spectra presented here are averages of 32 2048 point fast Fourier transforms, implying a 25-Hz frequency resolution. All overall sound pressure level (OASPL) data was further digitally filtered at 250 Hz to reduce the nonanechoic effects of the room at low frequencies.

## III. Results

### Mixing Results

Figure 2 shows the images of the jet 6.7 jet diameters downstream of the nozzle exit for a jet exit speed of 200 m/s ($M = 0.6$). All images were made with the 70-deg internal sweep angle generators. The white areas are smoke particles in the ambient air and the black areas are unmixed core flow. The gray areas are the regions in which ambient air has been entrained into and mixed with the core flow. The reference case refers to the case with no vortex generators, the CF out/in refers to the case of counter-rotating pairs with the common flow out the top and in the bottom, CF in/in refers to common flow in the top and bottom, and the symmetrical cases refer to the corotating vortices placed at either 45-or 90-deg intervals. A schematic of the vortices is above the respective pictures (except for the 45-deg symmetry case, where the picture is identical to the 90-deg symmetry case only with four more vortices). Finally, the percent improvement in mixing effectiveness over the reference case at this location is shown in each image.

Figure 2 clearly shows the benefits of the corotating vortices and of vortex strength on mass entrainment. The symmetry cases have visibly less untouched core flow (black) than do the counter-rotating cases (CF); this corresponds to as much as 10% difference in the measured mixing effectiveness improvement. Thus, the presence of the mirror (or counterrotating) vortex impedes the mixing capability, tending to displace the core more than mix it with the entrained flow. Further, one sees that the asymmetric counter-rotating pairs have a higher improvement in mixing, most likely because the symmetry provides a mirror in the horizontal plane as well as the vertical one. This becomes critical in the resulting acoustic field, where it appears that better mixing leads to less high-frequency noise and greater reduction of low-frequency noise. Further, as one might expect, the higher angle of attack (more circulation) entrains more ambient fluid in all cases. Interestingly, however, the increased circulation does not appear to increase the displacement of the core flow in the counter-rotating cases as one might expect from a potential flow analysis.

Closer examination of Fig. 2 shows the effect of the vortex growth. First, the counter-rotating pairs (CF cases) show a split in the unladen core (black). The vortex pairs tend to bring in ambient laden flow and push out the unladen core flow. In the symmetrical cases (out/out and in/in) this leads to an effective splitting of the core flow. The asymmetry of the common flow is evident in the out/in case, with core flow being pushed up (out) and ambient flow being pushed in by the vortices. Finally, one can see that the symmetric cases entrain much more ambient fluid, with the addition of the four more generators in the 45-deg symmetry case seeming to have little effect on the mixing. This is most likely related to the pairing of the eight corotating vortices into four.

### Acoustic Results

As one might expect, the streamwise vorticity alters not only the scalar and velocity fields, but also the acoustic field. The following results show a strong correlation between the mixing patterns and the resulting generated noise. In general, streamwise vorticity increased the high-frequency noise by generating more turbulence but reduced low-frequency noise by affecting the large-scale structures in the jet shear layer. The counter-rotating vortex pairs tended to increase the high frequency more and reduce the low frequency less than their corotating counterparts. That is, the symmetric cases had not only better mixing/entrainment, but better noise characteristics as well. Thus, our results show a strong correlation between the amount of entrainment and mixing and the resulting acoustic field.

*Acoustic Spectra*

Much of the effect of the generators lies in the origin of the sound. High-frequency noise tends to be omnidirectional, whereas the low-frequency noise is greatest in the axial or streamwise direction. This most likely results from the origin of the two sources; the high-frequency noise is generated by local turbulence, whereas the low-frequency noise comes from pressure fluctuations in the mean shear. Since the turbulence is random, the high-frequency noise should have no preferred direction. The fluctuations in the mean shear—a result of the characteristic roll structures—are not random and, therefore, one would expect a preferred direction. The vortex generators will generate more turbulence, thus increasing the high-frequency noise, but will affect the mean shear pressure fluctuations hence affecting the low-frequency noise.

The effect of the generators can be clearly seen in the increase in decibels for the 45-deg symmetry case, Fig. 3. The longitudinal axis is the frequency, and the vertical axis is the microphone position, with the 15-deg microphone on the top and the 105-deg microphone on the bottom. From this plot it is apparent that the generators increase the high-frequency noise of the jet but decrease the low-frequency noise. We found that, like the high-frequency noise, the decrease in low-frequency noise is also closely correlated to the vortex sign. Corotating pairs (45-deg and 90-deg symmetry cases) show a reduction in low-frequency noise, especially

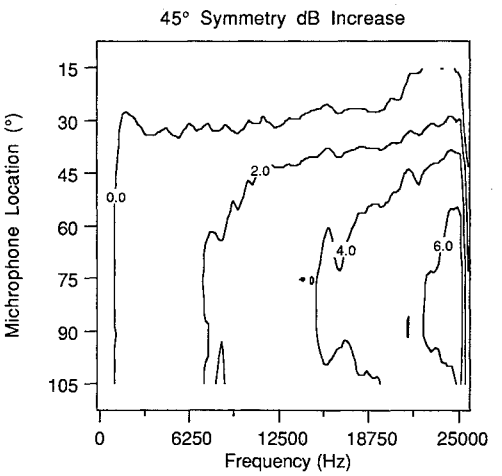


**Fig. 4 Overall sound pressure level.**

downstream of the jet (15-deg microphone). The actual relationship between the increased entrainment of the symmetry cases and the better acoustic characteristics deserves further study.

The counter-rotating pairs showed a much higher increase, showing little or no noise reduction in the low-frequency noise and as much as a 10-dB increase of the high-frequency noise downstream of the jet. Surks et al.[5] compares all of the cases in detail and showed that the azimuthal (or rotated) angle had little effect in the general acoustic trends and the generator angle of attack increased the high-frequency noise produced.

*Overall Sound Pressure Level*

The OASPL was obtained by integrating a sound spectrum over all frequencies, yielding a single measure indicative of the total amount of sound at a given spatial location. Figure 4 shows the total sound pressure level for the six different configurations for 20-deg angle of attack. One can see that the noise directly downstream of the nozzle exit is reduced by at least 2 dB by the vortex generators in all cases. Likewise, the off-axis noise is increased in all cases—sometimes by as much as 6 dB. Again, one can see that the better mixed symmetry cases perform better than the vortex pair cases. The effect of increasing the angle of attack corresponds to an increase in off-axis OASPL. The noise downstream of the nozzle remains relatively unaffected by the generator angle of attack. Similar results were found with the case of the rectangular nozzle,[1] although the increase in off-axis noise was not nearly as large.

## IV. Conclusion

In conclusion, the results of this work indicate that the acoustic and entrainment effects of introduced streamwise vortex structures are a strong function of vortex sign. Corotating vortices tended to entrain more fluid (up to 50%) without adding as much noise as their counterrotating counterparts. All introduced vorticity showed improved entrainment. Further, the corotating vortices reduced the low-frequency sound by as much as 3 dB, and increased the high-frequency noise by as much as 8 dB. Since most of the low-frequency noise is propagated downstream of the jet, these generator configurations decreased the OASPL downstream of the jet. Since most of the noise off to the side of the jet is high-frequency noise, the generators tended to increase the OASPL in this direction.

These results are qualitatively similar to the results found previously in a rectangular jet, however, the rectangular jet had a smaller increase in the high-frequency noise. This is most likely a result of the fact that the shear layer of the rectangular jet was substantially larger relative to the introduced vorticity (larger nozzle perimeter with same nozzle pressure ratio), implying that the turbulence generated by the vortex generators (same size) was a smaller portion of the total turbulence.

## Acknowledgments

This research was conducted in part under the McDonnell Douglas Independent Research and Development program and in part under Tufts University sponsorship. The authors are grateful to Nat Vignati, Joe Kroutil, Mike Meers, and Mark Carletti for assisting in these experiments and in the preparation of this manuscript.

## References

[1]Rogers, C. B., and Parekh, D. E., "Mixing Enhancement by and Noise Reduction of Streamwise Vortices in an Air Jet," *AIAA Journal*, Vol. 32, No. 3, 1994, pp. 464–471.

[2]Krishnappa, G., and Csanady, G. T., "An Experimental Investigation of the Composition of Jet Noise," *Journal of Fluid Mechanics*, Vol. 37, June 1969, pp. 149–159.

[3]Ahuji, K. K., and Brown, W. H., "Shear Flow Control by Mechanical Tabs," AIAA Paper 89-0994, March 1989.

[4]Samimy, M., Reeder, M., and Zaman, K., "Supersonic Jet Mixing Enhancement by Vortex Generators," AIAA Paper 91-2263, June 1991.

[5]Surks, P., Rogers, C. B., and Parekh, D., "The Effect of Streamwise Vorticity on the Mixing and Acoustic Characteristics of an Air Jet," Tufts Univ., TF-92-2, Medford, MA, Aug. 1992.

# Van Driest Transformation and Compressible Wall-Bounded Flows

P. G. Huang*
*Eloret Institute, Palo Alto, California 94303*
and
G. N. Coleman†
*NASA Ames Research Center, Moffett Field, California 94035*

## I. Introduction

EXCELLENT agreement was found by Huang et al.,[1] over a range of experiments, between zero pressure gradient (ZPG) compressible turbulent boundary-layer data and a refinement of the "Van Driest-I" density-weighted transformation.[2] The scheme's success supports Fernholz and Finley's[3] recommendation that the law of the wall for incompressible flows can be applied to the transformed velocity in a compressible flow. Zhang et al.,[4,5] however, have recently used experimental results from an earlier report by Fernholz and Finley,[6] and model calculations, to argue that the incompressible value of the von Kármán constant $\kappa = 0.41$ is observed only in the untransformed profiles—despite Fernholz and Finley's opposite conclusion. Zhang et al. have therefore raised some doubts regarding the transformation.

This Note examines the transformation validity question using results from direct numerical simulations (DNS) of supersonic, isothermal (cold) wall channel flow (Coleman et al.[7]). The DNS solutions include two cases: A) with Reynolds number $Re = 3000$, Mach number $M = 1.5$, and channel centerline-to-wall temperature ratio of $T_c/T_w = 1.38$, and B) with $Re = 4880$, $M = 3$, and $T_c/T_w = 2.47$. Here $M$ is based on bulk velocity and wall sound speed; $Re$ on bulk density, bulk velocity, channel half-width, and wall viscosity.[7] Dimensional analysis of the inner layer shows that the law of the wall can be described in terms of two nondimensional wall parameters,[8,9] $M_\tau = u_\tau/c_w \equiv u_\tau/\sqrt{(\gamma-1)\,c_p T_w}$ and $B_q = q_w/(\rho_w c_p u_\tau T_w)$ (where $c_p$ is the constant-pressure specific heat, $\gamma$ the specific heat ratio, $c_w$ the sound speed based on the wall temperature, $q_w$ the heat flux to the flow from the wall, and $u_\tau = \sqrt{\tau_w/\rho_w}$ with $\tau_w$ and $\rho_w$ the stress and density at the wall). Cases A and B are defined by $(M_\tau, B_q) = (0.08, -0.05)$ and $(0.12, -0.14)$. The two cases are therefore very different, with the former values of $M_\tau$ and $B_q$ being equivalent to a boundary layer at $M = 2.8$ on a moderately cooled wall with $T_w/T_{aw} \approx 0.4$ ($T_{aw}$ is the adiabatic wall temperature), and the latter equivalent to a layer at $M = 4.5$ over a strongly cooled wall given by $T_w/T_{aw} \approx 0.15$, both at momentum thickness $Re$ (based on freestream conditions) $Re_\theta \approx 4 \times 10^4$. (The $M_\tau$, $B_q$ dependence on freestream bulk parameters in ZPG compressible flows is discussed in Ref. 10.) The DNS results thus represent a wide parameter range and are ideally suited for our purpose of investigating the generality of the Van Driest transformation.

## II. Van Driest Law of the Wall

The Van Driest law of the wall can be derived from inner-layer similarity arguments[8,9] leading to "mixing-length" formulas for

Received Sept. 3, 1993; revision March 7, 1994; accepted for publication March 11, 1994. This paper is declared a work of the U.S. Government and is not subject to copyright protection in the United States.

*Research Scientist; Mailing address: M/S 229-1, NASA Ames Research Center, Moffett Field, CA 94035. Senior Member AIAA.

†Postdoctoral Fellow; currently at University of California at Los Angeles, Mechanical, Aerospace, and Nuclear Engineering Department, Los Angeles, CA 90024.